Scientific Research Publishing

Open Journal of Geology, 2026, 16(11), 832-847
https://www.scirp.org/journal/ojg
ISSN Online: 2161-7589
ISSN Print: 2161-7570

Tectonic Evolution of the Korhogo Greenstone Belt, Northern Côte d'Ivoire, West Africa

Krohognon Fofana[1], Koffi Raoul Teha[2*], Inza Coulibaly[3], Marc Ephrem Allialy[2]

[1]Laboratoire Sciences Environnementales et Technologies, UFR-Environnement, Université Jean Lorougnon Guede, Daloa, Côte d'Ivoire
[2]Laboratoire de Géologie, Ressources Minérales et Energétiques, UFR-STRM, Université Félix Houphouët-Boigny, Abidjan, Côte d'Ivoire
[3]Laboratoire Géosciences et Environnement, UFR-SGE, Université Nangui Abrogoua, Abidjan, Côte d'Ivoire
Email: *rkteha@hotmail.fr

How to cite this paper: Fofana, K., Teha, K.R., Coulibaly, I. and Allialy, M.E. (2026) Tectonic Evolution of the Korhogo Greenstone Belt, Northern Côte d'Ivoire, West Africa. *Open Journal of Geology*, **16**, 832-847.
https://doi.org/10.4236/ojg.2026.1611039

Received: October 29, 2026
Accepted: November 22, 2026
Published: November 25, 2026

Copyright © 2026 by author(s) and Scientific Research Publishing Inc.
This work is licensed under the Creative Commons Attribution International License (CC BY 4.0).
http://creativecommons.org/licenses/by/4.0/

Open Access

Abstract

The aim of this study is to characterize the deformation that has affected the Korhogo greenstone belt. To this end, we have drawn on an analysis of fieldwork. Structural data show that the study area is subject to polyphasic tectonics. The orientation of the principal stresses in the various deformation phases is reflected in the orientation of the schistosity and ductile structures. Four deformation phases, D1, D2, D3 and D4, have been identified. The shortening phase D1, oriented E-W to ENE-WSW, is responsible for schistosity S1. The major transpressive deformation phase D2, oriented NW-SE, generated schistosity S2, folding, quartz veins and a NE-SW-trending dextral shear zone. The compressive phase D3, oriented NE-SW, generated the schistosity S3 and late-stage quartz veins. Phase D4, oriented N-S, is accompanied by the superimposition of folds with subvertical axes. The schistosity S4 generated by phase D4 is oriented E-W.

Keywords

Korhogo Greenstone Belt, Structural Data, Four Deformation Phases

1. Introduction

The West African Craton (WAC) is one of the main records of paleoproterozoic crustal growth in Africa (Figure 1). In its southern part, the Baoulé-Mossi domain consists of volcano-plutonic, volcano-sedimentary and granitoid associations mainly attributed to the Eburnean cycle, the activity of which spans approximately 2.25 to 2.0 Ga [1]. These Birimian terrains record successive episodes of magma-

tism, sedimentation, deformation and metamorphism, which contributed to the building up and stabilization of the paleoproterozoic crust [2] [3]. Research on the WAC also emphasizes that no single tectonic model can describe the evolution of the Eburnean. For central Côte d'Ivoire, [2] propose an orogeny at a relatively high geothermal gradient, characterized by significant magmatic activity and deformation mechanisms that may include a vertical component. More recently, a study of the Bandamian volcanic cycle in the Bouaflé belt documented a late magmatic episode around 2.108 - 2.105 Ga, interpreted as a gradual transition from folding and thrusting to trans-tectonics [4]. These results illustrate the duration and complexity of the Eburnean evolution, but their extrapolation to Korhogo must be verified by local data.

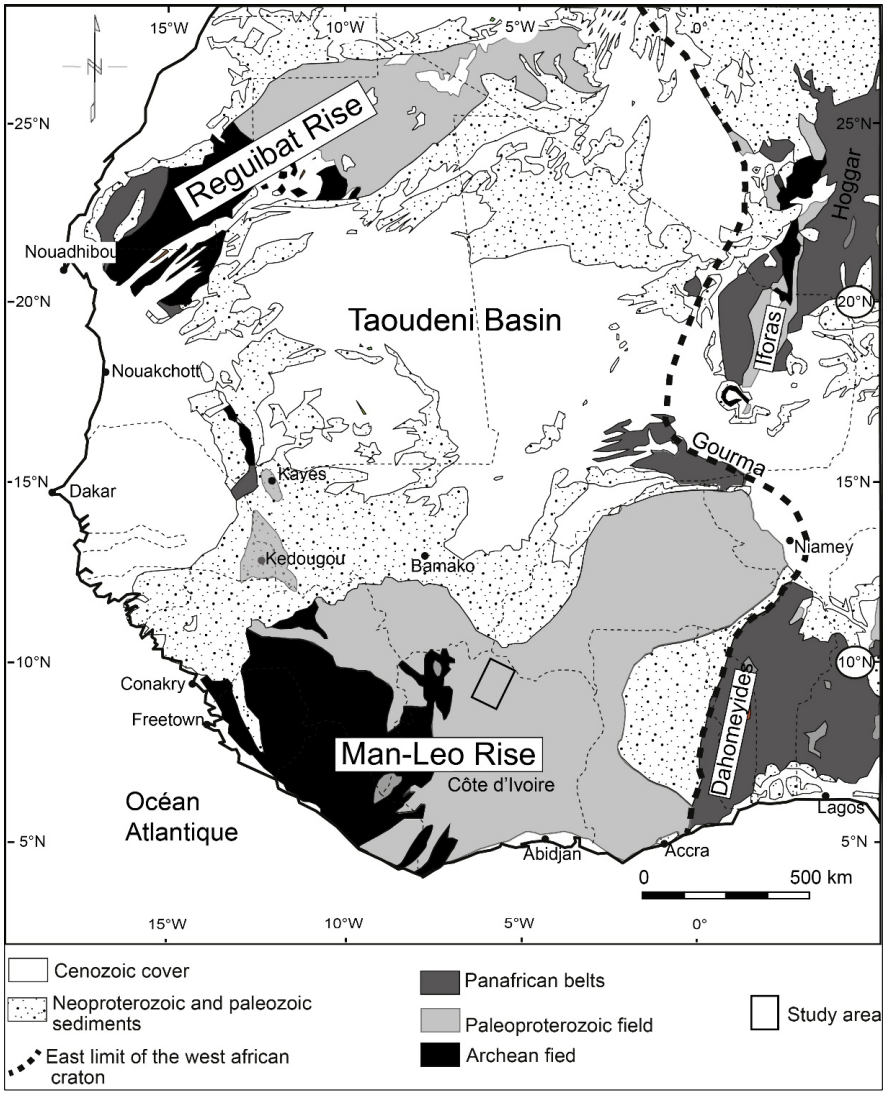


Figure 1. Simplified geological map of the West African craton [5].

In northern Côte d'Ivoire, the Korhogo region forms part of this Birimian complex and comprises volcanosedimentary formations associated with granitoids.

Regional studies indicate that the Birimian rocks of the Man Léo Shield were subject to a multi-phase structural evolution: early processes linked to magmatic emplacement and vertical movements were followed by trans-tectonic deformation, with a transition from ductile structures to more brittle ones [3]. These regional models provide a framework for comparison, but do not in themselves determine the chronology or kinematics specific to the Korhogo belt.

In this context, the study of the Korhogo greenstone belt aims to clarify the sequence of tectonic events that shaped the Birimian formations. Analysis of planar and linear fabric, folds, shear zones and their cross-cutting relationships allow us to test whether the observed structures result from progressive deformation or from several distinct episodes. The aim is therefore to construct a tectonic evolution model specific to Korhogo and to situate it within regional models of the eburnean orogeny of the West African Craton.

2. Regional Geological Context

The West African Craton (WAC) is traditionally subdivided into three distinct domains [6]: 1) to the north, the Reguibat Shield, outcropping in Algeria, Morocco and Mauritania, comprising Archean (3.0 - 2.7 Ga) and paleoproterozoic (~2 Ga) formations; 2) to the south, the Man-Leo Shield, formed by the Archean series of the Liberian Shield and the paleoproterozoic formations of the Baoulé-Mossi Domain, covering Ghana, Côte d'Ivoire, Guinea, southern Mali, Burkina Faso and western Niger (**Figure 1**). From a petrographic and geochronological perspective, the two ridges exhibit similarities. Situated between the two ridges; 3) the Kayes buttonhole in western Mali and the Kédougou buttonhole, located on either side of the Senegal-Mali border, outcrop within the Taoudéni Basin. These buttonholes are composed exclusively of the Birimian series.

3. Local Geological Context

The study area, the Korhogo-Niellé region, belongs to the Baoulé-Mossi domain and is situated within the Korhogo or Upper Bandama trough. This trough extends into Burkina Faso. It is oriented NNE-SSW. A large-scale reconnaissance interpretation shows that the geology of the rocks in this trough comprises a lithological assemblage of five formations [7]:

- syntectonic granitoids, including granitic gneisses;
- metavolcanites and metasediments;
- syntectonic basic intrusions, including metagabbros, actinolites and metadolerites, with a mineralogical assemblage dominated by tremolite-actinolite, plagioclases (andesine-albite), chlorite, epidote and quartz;
- post-tectonic granitoids;
- post-tectonic dolerite dykes;

The study area is bounded on both the western and eastern sides by granitoids. Between the granitoids, the host rocks consist of more or less metamorphosed volcano-sedimentary formations with a predominantly amphibolite facies (**Figure 2**).

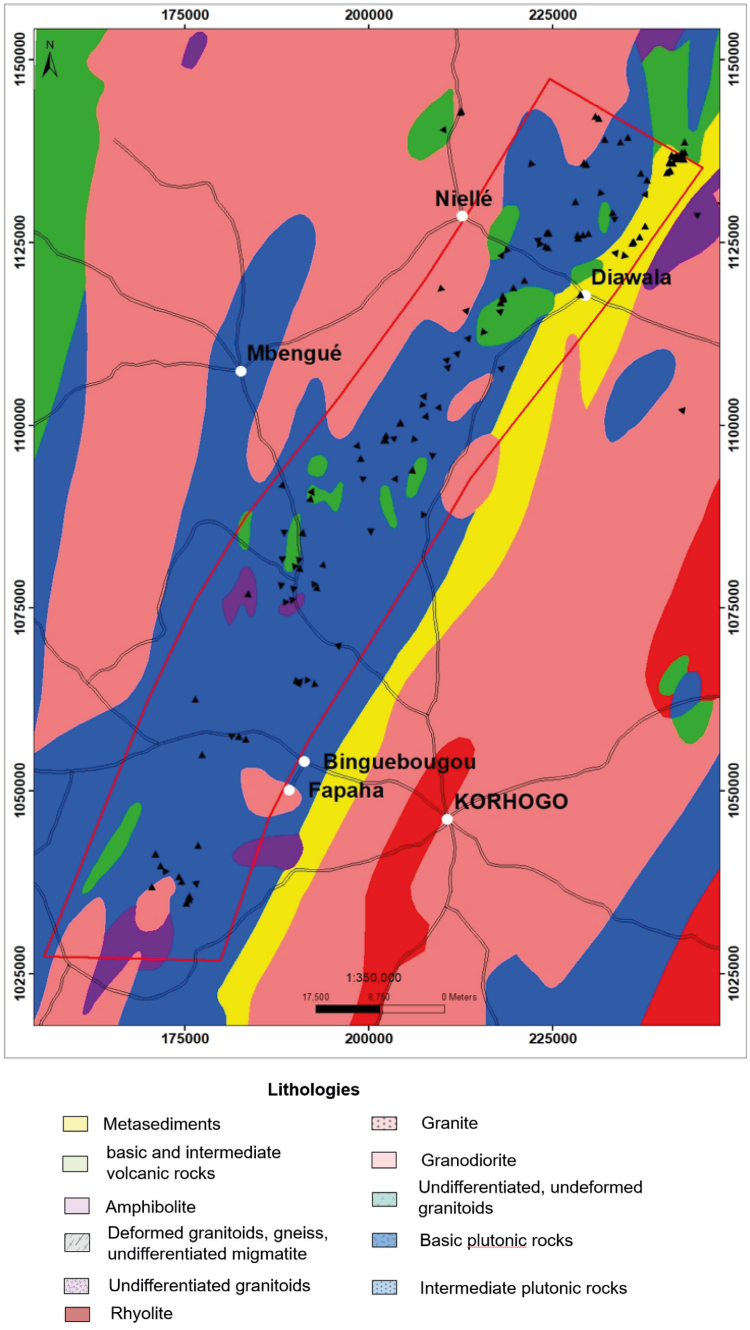


Figure 2. Geological map of Korhogo greenstone belt [8].

The metavolcanites and metasediments comprise fine-grained clastic rocks, abundant volcanoclastites, basaltic and andesitic lavas, rare rhyolites, fine- and coarse-grained sedimentary rocks, secondary tuffs, locally developed jaspoid cherts and rare conglomerates. This volcano-sedimentary complex contains small intrusive units of calc-alkaline granitoids, undifferentiated granitoids, and syn-tectonic and post-tectonic mafic intrusions (**Figure 2**).

The Korhogo Trough has historically been an area of prospecting activity, with several companies having carried out exploration work in a number of phases.

Among the companies that have worked in the trough are, amongst others, SODEMI, BHP Minerals, Randgold Resources, Resolute Limited (Ltd.), Occidental Gold and Semafo. These companies have carried out prospecting work on their various concessions, including airborne geophysical surveys. The work carried out varies from one area to another and includes regional to detailed mapping accompanied by sampling, the excavation of pits and trenches, and drilling (Auger, RAB, AC, RC, core).

4. Methodology

The structural analysis involved describing and interpreting all the structural features of the region at all scales (regional map scale, mesoscopic and microscopic scales). The aim is to provide a systematic structural framework that will enable the establishment of spatial and chronological relationships between the various structural features that have affected the rocks of the study area and to link them to the mechanical and geodynamic processes responsible for their development [9]. The kinematic aspect essentially involves the study of deformation fields (type, intensity and heterogeneity of finite deformation, deformation trajectories, symmetry of structures), whilst the mechanical aspect can be addressed through the analysis of the physical mechanisms of deformation at the microscopic and macroscopic scales. This method involves careful observation, description, analysis, and interpretation of the various types of folds, planar and linear structures, veins, and faults.

Structural measurements were taken at the various outcrops using a compass and an inclinometer. The structural analysis processes all these measurements from the studied area, which were obtained during the various geological mapping campaigns. The measurements are then exported as text to the OpenStereo software. This software enables the creation of stereograms from this data. The results of this analysis will enable us to identify and define the possible deformation phases that have affected the formations of the Senoufo Belt.

The measurements recorded are 19 for schistosity S1; 58 for schistosity S2; 17 for schistosity S3; and 11 for schistosity S4. The most deformed rocks are the metasediments and amphibolites. In the petrographic section, we present macroscopic and microscopic samples of these rocks from the Korhogo greenstone belt.

The aeromagnetic data were acquired during gold exploration work carried out by the Randgold mining company. As this data is confidential, we are unable to publish it in this article.

5. Petrography

5.1. Metasediments

The sediments observed in the study area consist of grauwackes and micaschists (**Figure 3(a)**, **Figure 3(b)**). These rocks are deformed and interspersed with numerous quartz veins.

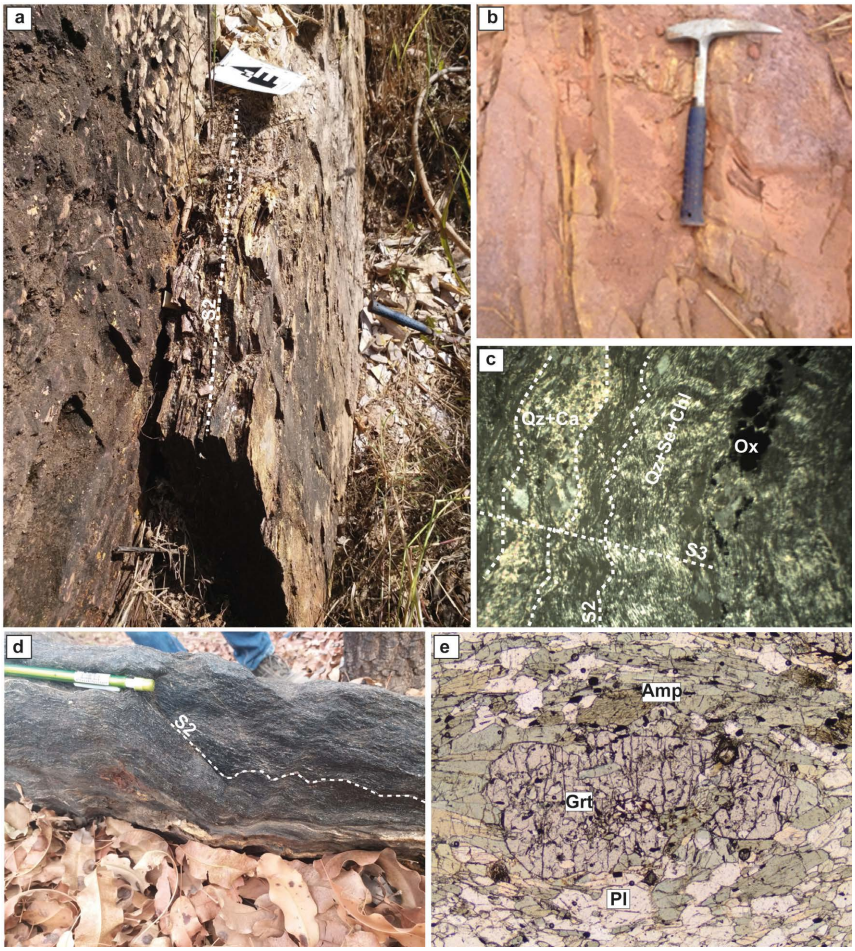


Figure 3. (a) Outcrop of mica schist showing S2 schistosity; (b) Outcrop of grauwacke; (c) A microphotograph showing the mineralogical composition of the mica schists; (d) An amphibolite outcrop showing crenulated S2 schistosity; (e) A microphotograph of the amphibolite showing phenocrysts of garnets, amphiboles and plagioclases.

The grauwackes found in the study area are massive, yellowish to reddish in colour, and composed of clear, rounded quartz grains set in a clayey cement (**Figure 3(b)**).

Macroscopic observation shows that the micaschists are very rich in micas (biotite and muscovite), which gives them a shiny, dark appearance on their cleavage surfaces. The most abundant minerals in the schistosity consist of sericite, chlorite and quartz (**Figure 3(c)**). Veins of carbonates are also present. These minerals are crenulated and oriented parallel to the schistosity plane. In addition to the schistosity, there is chemical and petrographic differentiation between the layers, resulting in a banded appearance.

5.2. Amphibolite

Amphibolites are massive, dark green, dense metamorphic rocks (**Figure 3(d)**). At outcrops, these rocks are highly deformed. They contain amphiboles, which are grouped in rod-like forms and constitute the bulk of the rock (75 percent,

Figure 3(e)). Garnets form the phenocrysts in amphibolites (Figure 3(e)). They are globular, cracked and vary in size. It contains inclusions of amphibole and opaque minerals. Plagioclase is less abundant (10 per cent, Figure 3(e)). It forms small crystals found in the interstices.

6. Structural Evolution

Based on the structural field data, we were able to identify four deformation events in the Korhogo greenstones belts, D1, D2, D3 and D4. The Eburnean orogeny is primarily reflected in deformation phases D1 and D2. The structural synthesis has enabled a chronology to be proposed for the genesis of the tectonic structures. In the study area, the descriptive and kinematic analysis of the main structures has allowed them to be grouped into four deformation phases according to their nature and geometric relationship. We shall describe the first two phases (D1 and D2) separately; however, there is a continuum of deformation from phase D1 to phase D2.

6.1. Deformation Phase D1

The structures that become apparent during the first phase of deformation are the S0 stratification and the S1 schistosity.

Within the study area, stratification surfaces were rarely observed. The S0 bedding is marked by bands of varying thickness, clearly defined within the metasediments. However, in most cases, the original geometry of S0 has been disrupted by subsequent tectonic events. The few measurements taken from contacts between the bands of the metasedimentary rocks indicate a general orientation of N170 with subvertical dips (Figure 4(a), Figure 4(b)).

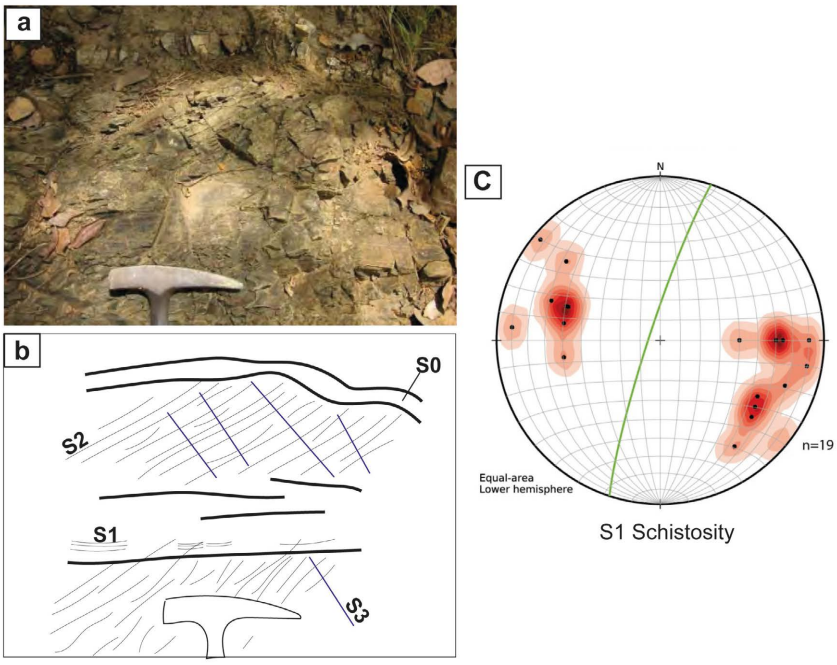


Figure 4. (a) Photograph showing the relationship between S0 stratification and S1, S2 and S3 schistosity. (b) Drawing based on the photograph (a). (c) S1 Schistosity stereonet plot.

Most metasediments and metavolcanites are affected by S1 schistosity. S1 is locally observed in areas of strong penetration by the second schistosity, S2. It is generally parallel to the S0stratification planes. Schistosity S1 has a NS to NNE-SSW strike with dips of 40˚ - 60˚ E/W, but also subvertical dips of 80˚ - 85˚ (**Figure 4(c)**). The stereographic projection indicates an average direction of N20˚ and a subvertical dip of 80˚ - 90˚ (**Figure 4(c)**).

Deformation phase D1 is poorly expressed due to subsequent tectonic events. The volcano-sedimentary units are affected by an initial schistosity S1, oriented N-S. Within the sedimentary units, S1 appears sub-conformable to the stratification S0. However, it is often difficult to assess S0 due to the intensity of subsequent deformation. No mineral lineations are associated with schistosity S1. D1 can be interpreted as an E-W shortening phase, responsible for the primary schistosity. D1 is also a flattening phase sub-orthogonal to stratification S0.

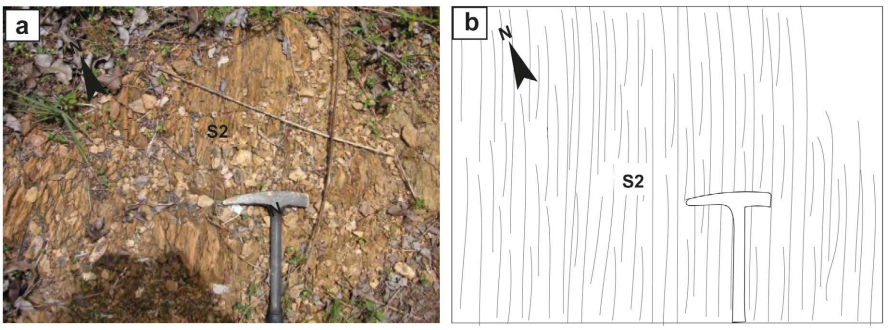
6.2. Deformation Phase D2

6.2.1. S2 Schistosity and Lineation

The planar S2 structure is the dominant feature throughout the study area. It probably corresponds to the peak of ductile deformation. This penetrating schistosity results in a more or less tight foliation exhibited by these rocks. This S2 structure is more pronounced in schists and amphibolites (**Figures 5(a)-(c)**). S2 schistosity very often occurs in the aforementioned incompetent and competent lithologies, in the form of penetrative schistosity or fracture cleavage (**Figures 5(a)-(c)**). Predominantly oriented NE-SW, S2 schistosity dips either 50˚ - 70˚ SE or NW, or 80˚ - 90˚ (subvertical dips).

Stereographic projections of measurements taken in the field indicate an average strike of N45˚ with a subvertical dip of 80˚ - 90˚ (**Figure 5(d)**). The angular relationship between S1 and S2 is relatively constant at ~25˚ (**Figure 5(d)**).

Across the study area, there is a striking scarcity of lineations in all their forms. Individual amphibole crystals have random rather than preferential orientations on the schistosity surfaces; this is consistent with the absence of any obvious stretch lineation. Where lineations are visible, they are formed by hinge lines of microfolds within the schistosity plane. Generally, these are crenulation lineations. A few measurements have been obtained and are grouped around a NE-SW direction, with steep pitches (80˚ - 85˚ NE). These subvertical lineations, highlighted by amphibole crystals, may be related to shear deformation.



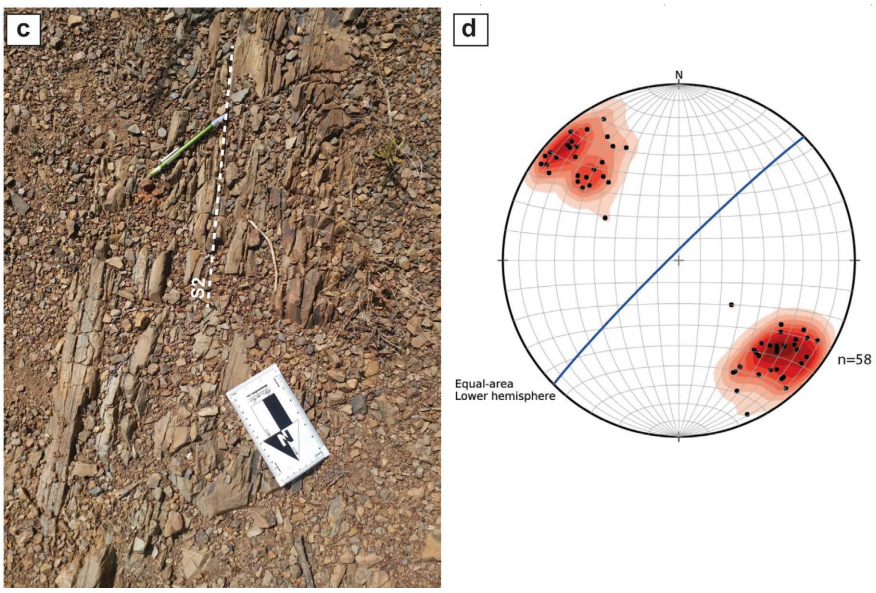


Figure 5. (a) Photograph showing S2 schistosity in metasediment; (b) Drawing based on the photograph (a); (c) Photograph showing S2 schistosity in amphibolite; (d) S2 Schistosity stereonet plot.

6.2.2. Folding Deformation

Fold tectonics generally occur in metasediments and amphibolites (**Figure 6**). The folds are localized and vary in amplitude (from centimeters to meters). The geometric relationships between the S0 bedding and the S2 schistosity of the few outcrops may indicate folding (**Figure 6(a)**, **Figure 6(b)**). S1 schistosity, discordant with the stratification, has developed to varying degrees in several metasediment beds (**Figure 6(c)**, **Figure 6(d)**). This schistosity is oriented approximately parallel to the axial planes of the associated folds. Mapping the orientation of this schistosity and the variation in its geometric asymmetry relative to the stratification should help to locate the fold hinges (**Figure 6(d)**).

The S1 schistosity in the metasediments and amphibolites is folded (**Figures 6(e)-(h)**). These folds exhibit axial planes oriented N50˚ - 65˚NW, subparallel to S2 (**Figure 6(e)**, **Figure 6(f)**). Locally, these P1 folds constitute a major deformation associated with the main schistosity S1. These folds display subvertical axes with steep dip (**Figure 6(g)**, **Figure 6(h)**).

6.2.3. Shear Zones and Faults

In the study area, aeromagnetic data reveal structures that could correspond to a broad shear zone. Shear planes have been mapped only within the volcanosedimentary units. Sudden changes in the orientation of schistosity within the same outcrop of metasediments were taken into account to establish the existence of a shear zone. These shear planes generally show dextral movement (**Figure 7(a)**). However, no obvious lineations were observed to indicate the direction of shear movement. Consequently, it is difficult to determine whether the shear movement was vertical, horizontal or oblique.

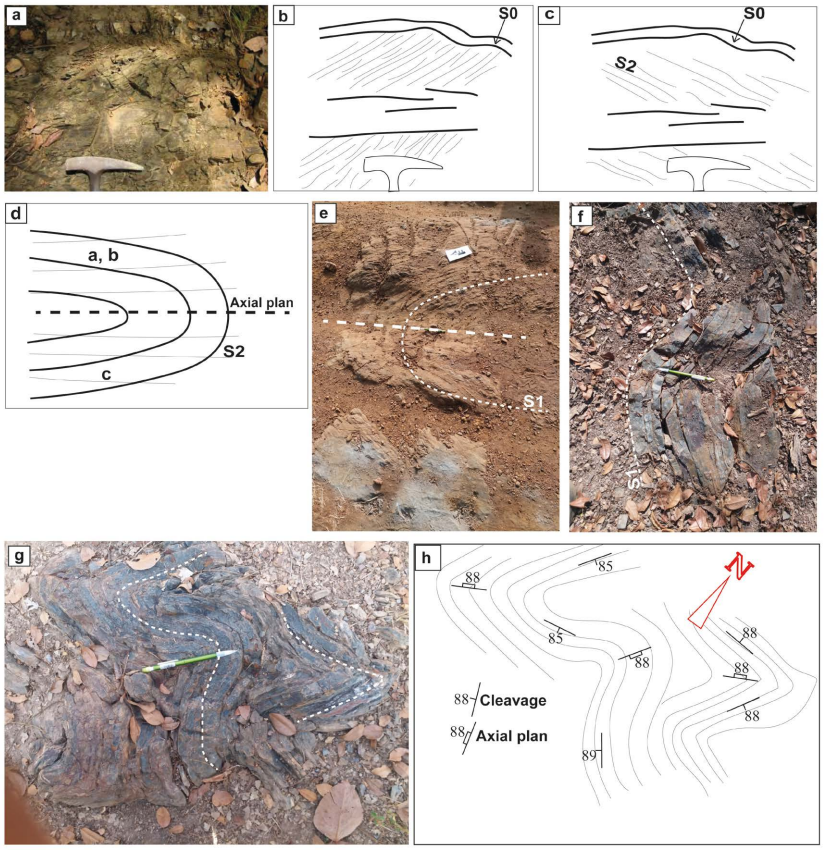


Figure 6. Macroscopic photographs of folding deformation in volcano-sedimentary rocks. (a)-(d) geometric relationships between the S0 bedding and S2 schistosity. (e) Folded metasedimentary rock; (f)-(g) Folded amphibolite rock with subvertical axes.

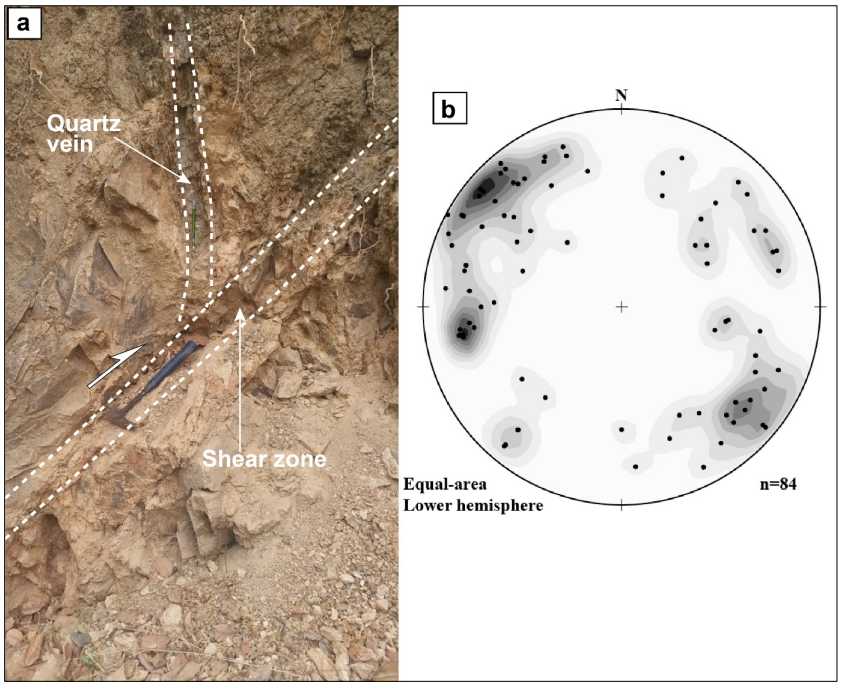


Figure 7. (a) Photograph of right-lateral shear deformation; (b) Shear stereonet plot.

The projection of the measurements of the shear planes that we considered reliable gives us two preferred orientations, with a main direction of NE-SW and a secondary direction of NW-SE (**Figure 7(b)**).

A second deformation phase, D2, is characterized by S2 schistosity, oriented NE-SW. S2 schistosity is highly penetrating within the amphibolites and takes the form of pressure-dissolution schistosity within the schist sequences. This phase may have been triggered by granitoid intrusions, as indicated by field and aeromagnetic observations. Deformation D2 is accompanied by folding in the metasediments, with axial planes oriented NE-SW. S2 Schistosity is associated with subvertical lineation. D2 is a compressive phase, occurring simultaneously with numerous hydrothermal alterations manifested as NE-SW-trending shear quartz veins and NW-SE-trending extension veins. The D2 deformation phase is accompanied by a NE-SW-trending shear zone with right-lateral slip. D2 is therefore a NW-SE to E-W transpressional phase. The transpression is responsible for the verticalization of the volcano-sedimentary units and the presence of the local subvertical lineation.

6.3. Deformation Phase D3

The main S2 schistosity is cut by a secondary S3 schistosity (**Figure 8(a)**, **Figure 8(b)**). This third schistosity exhibits schistosity planes separated by a few millimeters or more, delineating volumes free of schistosity. This is a fracture cleavage that is non-penetrating and affects S2. The stereograms and mean planes of S3 schistosity are shown in **Figure 8**. A preferential orientation of N110 to N150 is defined, with mean to subvertical dips of 50˚ to 80˚ to the NE or NW (**Figure 8(d)**).

Furthermore, the deformed rocks exhibit crenulation schistosity with left-lateral manifestations (**Figure 8(c)**). In this crenulation schistosity, the former S2 schistosity has been folded and reoriented by shear deformation. This new S3 schistosity, which penetrates the tectonites, manifests as microfolds intersecting the S2 schistosity and is oriented N110. NE-SW-trending extension veins form within the planes of the S2 schistosity during phase D3. Deformation phase D3 is therefore a NE-SW-trending compressional phase.

6.4. Deformation Phase D4

Furthermore, the secondary schistosity S2 is affected by a fourth schistosity, designated S4. The overall orientation of schistosity S4 is E-W with a mean dip directed towards the S (**Figure 8(a)**, **Figure 8(b)**). This is generally a spaced cleavage that occurs in volcanosedimentary formations as a series of fractures locally intersecting schistosity S2 (**Figure 8(a)**, **Figure 8(b)**). The mean plane of schistosity S4 is N85 with a subvertical dip of 80˚ - 90˚ (**Figure 8(e)**).

The fourth deformation phase, D4, is responsible for an E-W-trending spaced schistosity S4, which cuts across S1 and S2. The folds generated during D2 are refolded during the D4 phase, thus forming superimposed folds with subvertical axes. D4 is a compressive deformation phase, oriented N-S.

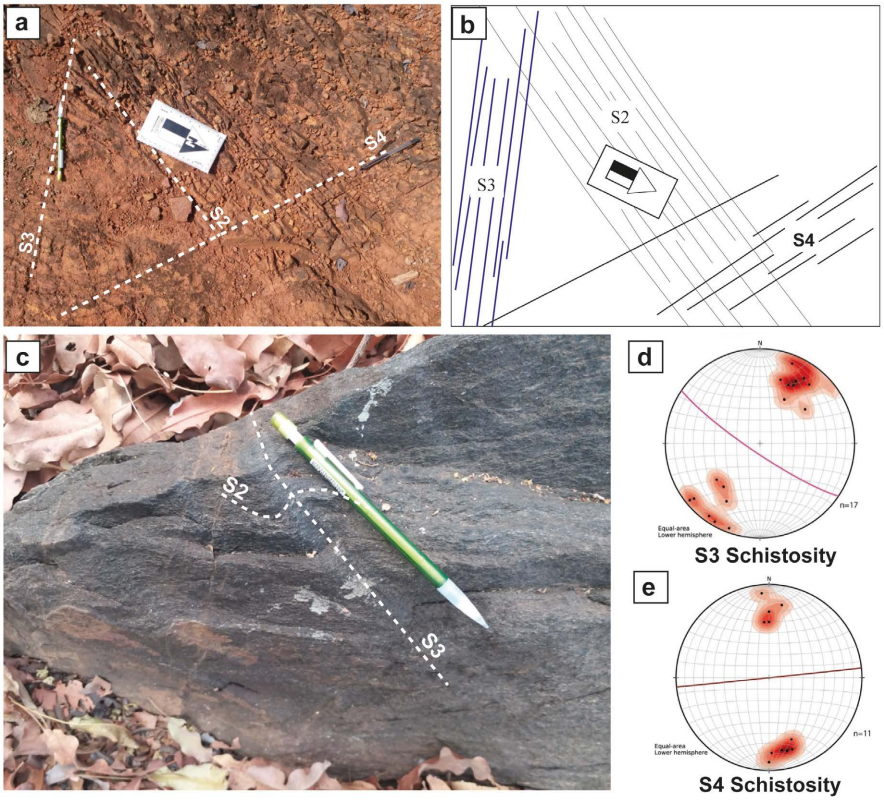


Figure 8. Structures of deformation phases D3 and D4. (a) Relationship between S2, S3 and S4; (b) Drawing based on the photograph (a); (c) Crenulation schistosity S3; (d) S3 schistosity stereonet plot; (e) S4 schistosity stereonet plot.

7. Quartz Veins

The rocks of the Korhogo greenstones belt have been cut by several generations and types of quartz veins. In general, these veins run subparallel to the S1 schistosity, although others intersect it (**Figure 7(a)**). Seventy-one measurements were taken on the veins. When entered into the OpenStereo software, the dominant trend identified is NE-SW with generally subvertical dips of 70˚ - 90˚. Secondary trends of NS, NNE-SSW and NW-SE are also observable (**Figure 7(a)**). Two types of veins or vein networks are distinguished:

- extension veins, which form under conditions of pure extension and low stress. These veins are found within the shear zone or between two shear zones and are subparallel to the main schistosity S1 in the majority of cases (**Figure 7(a)**).
- shear veins, found in schists and under compression and high differential stresses.

8. Discussion

8.1. Tectonic Scenario

Structural analysis has shown that the Korhogo belt was subjected to ductile-brittle deformation. Four major deformation phases affected the rocks.

Phases D1, D2, D3 and D4 are chronologically distinct. The first phase, D1 (E-

W to ENE-SSE), corresponds to a compressive phase responsible for the flattening that generated schistosity S1. This phase is very poorly represented, as is the case in other regions of Côte d'Ivoire [10] [11] and in southern Burkina Faso [1].

The second deformation phase is interpreted as a NO-SE transpressional phase. This deformation phase gave rise to schistosity S2, folding, quartz veins and NE-SW right-lateral shear zones. The S2 schistosity, oriented at N45˚, is highly penetrating and takes the form of a flow schistosity in the central part of the shear zone. The structures observed in the study area, notably the shear zones, schistosity, folds and quartz veins, demonstrate that this area is a shear corridor [12]. These zones constitute good prospects for mineral exploration, as they are characterized by these distinctive structures; indeed, they represent zones of significance for the formation of ore deposits [13].

The shear zones, which develop predominantly in areas of high anisotropy, are consistent with a right-lateral shear movement. Within the study area, the NE-SW-trending shear zones are the main structures hosting gold mineralization.

Indeed, in these mylonitisation zones, the tectonic structures acquire a permeability that turns them into effective conduits for hydrothermal fluids. Shear deformation has therefore facilitated the channeling of fluids into areas of high permeability.

The NE-SW shear zones also host gold mineralization in certain regions of Côte d'Ivoire, notably at Agbahou [14], Afema [15] and even in West Africa, specifically at Sabodala in Senegal [16], at Abawso in Ghana [17] and at Taparko in Burkina Faso [18].

The D3 deformation phase is a compressional phase oriented NE-SW. It is responsible for the NW-SE S3 schistosity and the late-stage quartz veins. The NW-SE structures are interpreted as channels controlling the distribution of gold mineralization in the Ashanti Belt [19]. They transported and trapped hydrothermal fluids.

The N-S-trending D4 deformation phase is accompanied by the superimposition of folds. The S4 schistosity generated by D4 is oriented E-W. The direction of this schistosity suggests a rotation of the principal stress, with N-S shortening. This shortening results in the initial right-lateral shear being replayed as a left-lateral shear during D4. This latter phase corresponds to the D4 deformation phase described by [1]. The structures of the D4 phase acted as conduits during the formation of the NE-SW mineralization. However, neither the structures of the D3 deformation phase nor those of the D4 deformation phase contain any traces of gold mineralization. Furthermore, the NW-SE and E-W structures are not deep-seated structures.

All of these structural data have enabled us to propose a new geological map of the Korhogo greenstone belt, which highlights new lithologies as well as new structures, in contrast to that of [9]. Indeed, at the lithological level, our work has revealed basic and intermediate volcanic rocks (volcanic lavas and volcaniclastics) interbedded with metasediments (argillite, sandstone, conglomerate). Our work has also enabled us to classify certain granitoids as granites and granodiorites, and

to identify additional lithological units (amphibolite and rhyolite). Structurally, our work reveals lithological units generally oriented NNE-SSW in line with the major structures of the rift valley, as well as late-stage NS and E-W structures. We have also identified pressure shadow zones around the intrusions. This new map will provide a better structural and geological understanding, enabling more targeted exploration work. Indeed, prospective zones such as lithological contacts, structural crossings, areas where structures change direction, and pressure shadow zones around intrusions—which generally represent areas favorable to the formation of mineralization—have been identified.

8.2. Tectonic and Gold Mineralization Event

Most, if not all, of these structures probably developed during regional metamorphism and regional NW-SE shortening at the cratonic scale. Such deformation occurred throughout the Birimian period during the inversion of the major sedimentary basins, and perhaps earlier in the mafic volcanic rocks of the belts, before the formation of the basins [1] [20]. D2 deformation, oriented NW-SE, is also documented in western Burkina Faso and is thought to correspond to the D2 phase [1] and in Côte d'Ivoire [21]. Gold mineralization is often associated with these regionally scaled S2 shear zones [22]-[25]; the Mana mine, situated to the north of the Houndé belt, is a typical example of this [26].

9. Conclusion

The structural analysis shows that the study area is affected by polyphasic tectonics. The orientation of the principal stresses in the various deformation phases is characterized by the geometry of the schistosity and ductile structures. Four deformation phases—D1, D2, D3 and D4—have been identified. The D1 shortening phase, oriented E-W to ENE-WSW, is responsible for schistosity S1. D1 is suborthogonal to stratification S0. The major deformation phase is phase D2, which generated schistosity S2, folding, quartz veins and a NE-SW-trending right lateral shear zone. The compressive phase D3, oriented NE-SW, gave rise to schistosity S2 and late-stage quartz veins. The deformation phase D4, oriented N-S, is accompanied by the superimposition of folds with subvertical axes. The schistosity S4 generated by D4 is oriented E-W.

Acknowledgements

This work is the result of thesis work by Fofana K. We would like to thank Geology department of Université Félix Houphouët-Boigy-Abidjan for his involvement in the production of this paper.

Author Contributions

Conceptualization, Krohognon Fofana and Koffi Raoul Teha; methodology, Krohognon Fofana and Koffi Raoul Teha; software, Krohognon Fofana; validation, Krohognon Fofana, Koffi Raoul Teha, Inza Coulibaly, Marc Ephrem Allialy;

formal analysis, Krohognon Fofana, Koffi Raoul Teha, Inza Coulibaly; resources, Krohognon Fofana; data curation, Krohognon Fofana; writing—original draft preparation, Krohognon Fofana, Koffi Raoul Teha, Inza Coulibaly; writing—review and editing, Krohognon Fofana, Koffi Raoul Teha, Inza Coulibaly; visualization, Krohognon Fofana, Koffi Raoul Teha, Inza Coulibaly; supervision, Marc Ephrem Allialy; project administration, Krohognon Fofana; funding acquisition, Krohognon Fofana. All authors have read and agreed to the published version of the manuscript.

Conflicts of Interest

The authors declare no conflicts of interest regarding the publication of this paper.

References

[1] Baratoux, L., Metelka, V., Naba, S., Jessell, M.W., Grégoire, M. and Ganne, J. (2011) Juvenile Paleoproterozoic Crust Evolution during the Eburnean Orogeny (~2.2-2.0 Ga), Western Burkina Faso. *Precambrian Research*, **191**, 18-45. https://doi.org/10.1016/j.precamres.2011.08.010

[2] Vidal, M., Gumiaux, C., Cagnard, F., Pouclet, A., Ouattara, G. and Pichon, M. (2009) Evolution of a Paleoproterozoic "Weak Type" Orogeny in the West African Craton (Ivory Coast). *Tectonophysics*, **477**, 145-159. https://doi.org/10.1016/j.tecto.2009.02.010

[3] Lompo, M. (2010) Paleoproterozoic Structural Evolution of the Man-Leo Shield (West Africa). Key Structures for Vertical to Transcurrent Tectonics. *Journal of African Earth Sciences*, **58**, 19-36. https://doi.org/10.1016/j.jafrearsci.2010.01.005

[4] Mériaud, N., Thébaud, N., Masurel, Q., Hayman, P., Jessell, M., Kemp, A., *et al.* (2020) Lithostratigraphic Evolution of the Bandamian Volcanic Cycle in Central Côte d'Ivoire: Insights into the Late Eburnean Magmatic Resurgence and Its Geodynamic Implications. *Precambrian Research*, **347**, Article 105847. https://doi.org/10.1016/j.precamres.2020.105847

[5] Béziat, D., Bourges, F., Debat, P., Lompo, M., Martin, F. and Tollon, F. (2000) A Paleoproterozoic Ultramafic-Mafic Assemblage and Associated Volcanic Rocks of the Boromo Greenstone Belt: Fractionates Originating from Island-Arc Volcanic Activity in the West African Craton. *Precambrian Research*, **101**, 25-47. https://doi.org/10.1016/s0301-9268(99)00085-6

[6] Bessoles, B. (1977) Géologie de l'Afrique, le craton ouest africain Mém. Bureau de Recherches Géologiques et Minières.

[7] Turner, P., Hall, R.P., Hughes, D.J. and Whalley, J.S. (1993) The Sediment-Dominated Boundiali-Bagoé Supracrustal Belt and Neighbouring Granitic Rocks, Northern Côte d'Ivoire, West Africa: A Tarkwaian Connection? *Journal of African Earth Sciences* (*and the Middle East*), **17**, 1-11. https://doi.org/10.1016/0899-5362(93)90017-k

[8] Sems Exploration (2012) West Africa Geological Map. West Africa Geological Consultancy Group. https://www.sems-exploration.com

[9] Dominique F.D.L., Pascale L., Souloumiac P. and Adrien, F.D.L. (2019) Objets et structures géologiques en trois dimensions. Edition Dunod, 168 p.

[10] Teha, K.R. (2019) Les Formations Éburnéennes du Sud-ouest du bassin de la Comoé et du secteur de Singrobo (Sud de la Côte d'Ivoire): Pétrologie, Analyse structurale et Magmatisme associé. Doctoral Thesis, Université Félix Houphouët-Boigny.

[11] Pria, K.K.J.M. (2021) Caractéristiques pétrographique, structurale et géochimique du complexe granito-gneissique du kan (région est de Toumodi, centre de la côte d'Ivoire): Implication dans la géodynamique des formations Paléoprotérozoïque du craton ouest-africain. Thèse de Doctorat, Université Félix Houphouët-Boigny.

[12] Passchier, W. and Trouw, R.A.J. (1998) Microtectonic. Springer.

[13] Sonnendrucker, P. (1969) Etude de synthèse sur l'or en Côte d'Ivoire, rapport de fin de mission, SODEMI, Abidjan, rapport No. 222, 127p.

[14] Houssou, N.N. (2013) Etude pétrologique, structurale et métallogénique du gisement aurifère d'Agbahou, Divo, Côte d'Ivoire. Doctorat, Université Félix Houphouët-Boigny.

[15] Assie, K.E. (2008) Lode Gold Mineralization in the Paleoproterozoic (Birimian) Volcano Sedimentary Sequence of Afema Gold District, Southeastern Côte d'Ivoire. Doctoral Thesis, Faculty of Energy and Economic Sciences Technical University of Clausthal.

[16] Sylla, M. and Ngom, P.M. (1997) Le Gisement d'or de Sabodala (Sénégal Oriental): Une Minéralisation Filonienne d'Origine Hydrothermale Remobilisée par une Tectonique Cisaillante. *Journal of African Earth Sciences*, **25**, 183-192. https://doi.org/10.1016/s0899-5362(97)00097-3

[17] Wille, S.E. and Klemd, R. (2004) Fluid Inclusion Studies of the Abawso Gold Prospect, Near the Ashanti Belt, Ghana. *Mineralium Deposita*, **39**, 31-45. https://doi.org/10.1007/s00126-003-0380-1

[18] Bourges, F., Debat, P., Tollon, F., Munoz, M. and Ingles, J. (1998) The Geology of the Taparko Gold Deposit, Birimian Greenstone Belt, Burkina Faso, West Africa. *Mineralium Deposita*, **33**, 591-605. https://doi.org/10.1007/s001260050175

[19] Feybesse, J.L., Billa, M., Guerrot, C., Duguey, E., Lescuyer, J., Milesi, J., *et al.* (2006) The Paleoproterozoic Ghanaian Province: Geodynamic Model and Ore Controls, Including Regional Stress Modeling. *Precambrian Research*, **149**, 149-196. https://doi.org/10.1016/j.precamres.2006.06.003

[20] Allibone, A., Teasdale, J., Cameron, G., Etheridge, M., Uttley, P., Soboh, A., *et al.* (2002) Timing and Structural Controls on Gold Mineralization at the Bogoso Gold Mine, Ghana, West Africa. *Economic Geology*, **97**, 949-969. https://doi.org/10.2113/gsecongeo.97.5.949

[21] Siagné, Z.H., Tahar, A., Alain, N.K., N'Guessan, N.H. and Wilfried, D. (2021) Analyse Structurale de la Déformation Dans Les Granitoïdes Éburnéens De La Région De Doropo (Nord-Est De La Côte d'Ivoire). *European Scientific Journal*, **17**, 157-172. https://doi.org/10.19044/esj.2021.v17n29p157

[22] Milési, J.P., Feybesse, J.L., Ledru, P., Dommaget, A., Ouédraogo, M.F., *et al.* (1989) Les minéralisations aurifères de l'Afrique de l'Ouest. *Chronique Recherche Minière*, **497**, 3-98.

[23] Milési, J.P., Ledru, P., Ankrah, P., Johan, V., Marcoux, E. and Vinchon, C. (1991) The Metallogenic Relationship between Birimian and Tarkwaian Gold Deposits in Ghana. *Mineralium Deposita*, **26**, 228-238. https://doi.org/10.1007/bf00209263

[24] Milési, J.P., Ledru, P., Feybesse, J.L., Dommanget, A. and Marcoux, E. (1992) Early Proterozoic Ore Deposits and Tectonics of the Birimian Orogenic Belt, West Africa. *Precambrian Research*, **58**, 305-344. https://doi.org/10.1016/0301-9268(92)90123-6

[25] Castaing, C., Billa, M., Milési, J.P., Thiéblemont, D., *et al.* (2003) Notice explicative de la carte géologique et miniére du Burkina Faso à 1/1000000. BRGM and BUMIGEB.

[26] Ilboudo, H., Abraham Traoré, S., Sawadogo, S., Nonguierma, B. and Toubania, S. (2018) Geology and Gold Occurrences of the gombélédougou paleoproterozoic terrane, houndé belt in burkina faso (West-Africa). *Journal des sciences*, **18**, 1-12.